Human Molecular Genetics, 2011, Vol. 20, No. 5 ***917–926***
doi:10.1093/hmg/ddq530
Advance Access published on December 6, 2010

Esrrg functions in early branch generation of the ureteric bud and is essential for normal development of the renal papilla

Rachel Berry[1,†], Louise Harewood[1,†,‡], Liming Pei[2], Malcolm Fisher[1], David Brownstein[3], Allyson Ross[1], William A. Alaynick[2], Julie Moss[1], Nicholas D. Hastie[1], Peter Hohenstein[1], Jamie A. Davies[4], Ronald M. Evans[2] and David R. FitzPatrick[1,*]

[1]MRC Human Genetics Unit, Institute of Genetic and Molecular Medicine, Western General Hospital, Edinburgh EH4 2XU, UK, [2]The Salk Institute, Howard Hughes Medical Institute, 10010 No. Torrey Pines Road, La Jolla, CA 92037, USA, [3]Molecular Pathology, Queen's Medical Research Institute, University of Edinburgh, Edinburgh EH16 4TJ, UK and [4]Centre for Integrative Physiology, University of Edinburgh, George Square, Edinburgh, UK

Received August 25, 2010; Revised and Accepted December 1, 2010

Congenital anomalies of the kidney and urinary tract (CAKUTs) are common disorders of human development affecting the renal parechyma, renal pelvis, ureter, bladder and urethra; they show evidence of shared genetic aetiology, although the molecular basis of this remains unknown in the majority of cases. Breakpoint mapping of a *de novo*, apparently balanced, reciprocal translocation associated with bilateral renal agenesis has implicated the gene encoding the nuclear steroid hormone receptor ESRRG as a candidate gene for CAKUT. Here we show that the Esrrg protein is detected throughout early ureteric ducts as cytoplasmic/sub-membranous staining; with nuclear localization seen in developing nephrons. In 14.5–16.5 dpc (days post-conception) mouse embryos, Esrrg localizes to the subset of ductal tissue within the kidney, liver and lung. The renal ductal expression becomes localized to renal papilla by 18.5 dpc. Perturbation of function was performed in embryonic mouse kidney culture using pooled siRNA to induce knock-down and a specific small-molecule agonist to induce aberrant activation of Esrrg. Both resulted in severe abnormality of early branching events of the ureteric duct. Mouse embryos with a targeted inactivation of Esrrg on both alleles ($Esrrg^{-/-}$) showed agenesis of the renal papilla but normal development of the cortex and remaining medulla. Taken together, these results suggest that Esrrg is required for early branching events of the ureteric duct that occur prior to the onset of nephrogenesis. These findings confirm ESRRG as a strong candidate gene for CAKUT.

INTRODUCTION

Formation of the primary nephric duct as symmetric bilateral cords of epithelial cells (1) at 22 gestational days in human embryos is the first evidence of kidney development. A transient embryonic kidney, the mesonephros, then forms along the long axis of the nephric duct (2) with the definitive kidney or metanephros forming via an outgrowth of the distal nephric duct, the ureteric bud, which then undergoes extensive branching and induces the surrounding mesoderm to form glomeruli and nephrons (3,4). The first 6–10 generations of ureteric branching events will form the pelvis and calyces and are not associated with nephrogenesis (5). The molecules determining the position of the boundaries between ureter and renal pelvis or between renal papilla and collecting duct fate have not yet been identified.

*To whom correspondence should be addressed. Tel: +44 1314678423; Email: david.fitzpatrick@hgu.mrc.ac.uk
†The authors wish it to be known that, in their opinion, the first two authors should be regarded as joint First Authors.
‡Present address: Center for Integrative Genomics, University of Lausanne, Genopode Building, UNIL-Sorge, Lausanne CH 1015, Switzerland.

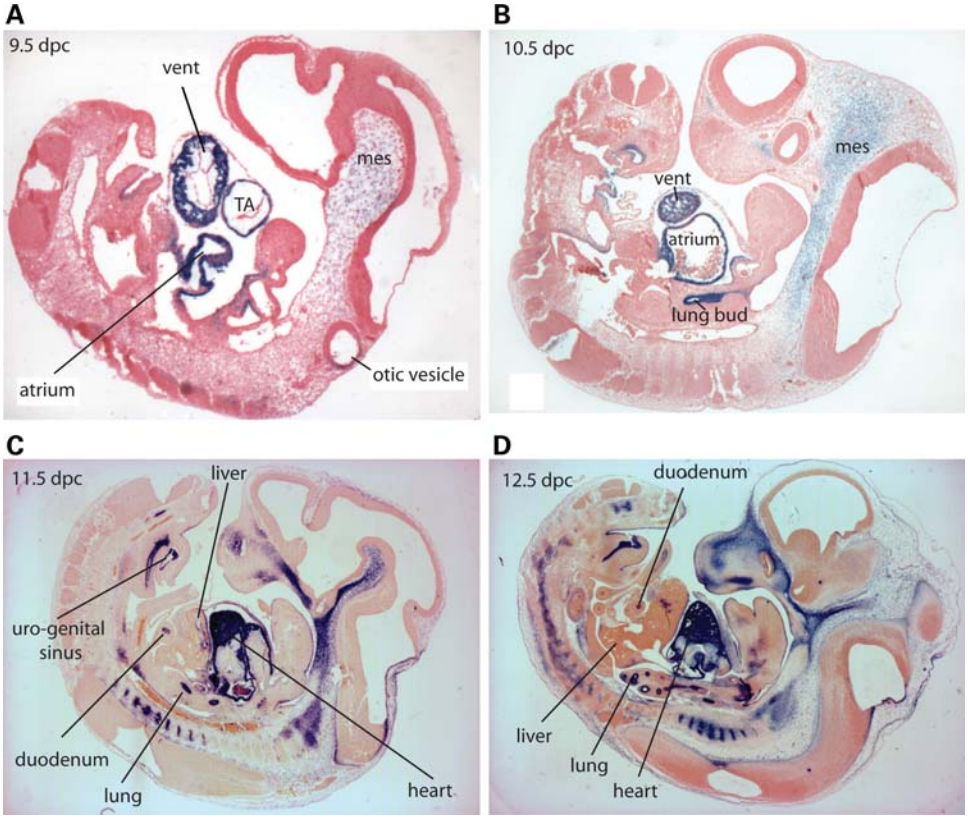

Figure 1. Esrrg immunohistochemistry on sectioned mouse embryos. Photomicrographs of Esrrg immunohistochemical staining of saggital sections of mouse embryos counterstained with eosin (pink) and signal detected with NBT/BCIP (blue). (**A**) 9.5 dpc embryo showing strong staining in the primitive ventricle, atrium and TA. There is also expression seen in the head mesenchyme (mes) and faint staining in the dorsal aspect of the otic vesicle. (**B**) 10.5 dpc embryo showing continued strong staining in the developing heart. There is also a prominent signal in the developing lung bud and expression in the head mesenchyme. (**C**) 11.5 dpc embryo showing strong expression in the heart, lung and condensing mesenchyme in the head. New regions of strong staining are now apparent in the urogenital sinus and the duodenum. Faint expression can be seen in the ducts within the liver. (**D**) 12.5 dpc embryo showing a very similar expression pattern to 11.5 dpc.

Congenital anomaly of the kidney and urinary tract (CAKUT) is a term used to describe a common and medically important group of developmental disorders of the kidney, renal pelvis, ureter, bladder and urethra. Malformations of these anatomically distinct structures show evidence of shared aetiology on the basis of coexistence of different malformations in individual cases, family studies and animal models. The most severe forms of CAKUT, bilateral renal agenesis/hypoplasia/dysplasia (BRAHD), are malformations of the renal parenchyma that are usually lethal. We recently reported breakpoint mapping of a *de novo*, apparently balanced reciprocal translocation, t(1;2)(q41;p25.3) (6), associated with non-syndromal bilateral renal agenesis. At the 1q41 breakpoint, aberrant *cis*-regulation of *ESRRG* was identified as a candidate mechanism for BRAHD in this case (7) on the basis of proximity to the breakpoint and strong expression in the developing kidney assess by whole-mount *in situ* hybridization using an antisense riboprobe. *ESRRG* encodes an orphan nuclear steroid hormone receptor previously known as estrogen-related receptor gamma. No endogenous ligand is known for ESRRG and ligand-binding may not be essential for at least some aspects of transcriptional activity (8). However, specific small molecule agonists (9–12) and antagonists (8) of ESRRG have been identified.

Here we functionally assess *ESRRG* as a candidate gene for CAKUT. We show that Esrrg expression is limited to proximal (i.e. closest to the ureter) ductal tissue, which is derived from the early generations of branching of the ureteric bud. Both activation and inactivation of this nuclear steroid hormone receptor result in severe abnormality of early branching events in cultured kidneys. Analysis of mouse embryos with a targeted inactivation of *Esrrg* on both alleles ($Esrrg^{-/-}$) showed an unusual and previously unsuspected anomaly of renal papillary agenesis.

RESULTS

Expression of Esrrg during mouse embryogenesis

Immunohistochemical analysis of Esrrg in wild-type embryos showed strong and persistent staining in the primitive ventricle, atrium and truncus arteriosus (TA) of the developing heart from 9.5 dpc (Fig. 1). Strong expression is also seen in a subset of the head mesenchyme from 9.5 to 12.5 dpc. Faint staining in the dorsal aspect of the otic vesicle is detectable at 9.5 dpc. From 10.5 dpc, strong staining is seen in the branching bronchial tree of the developing lung. By 11.5 dpc, strong staining is also apparent in the urogenital

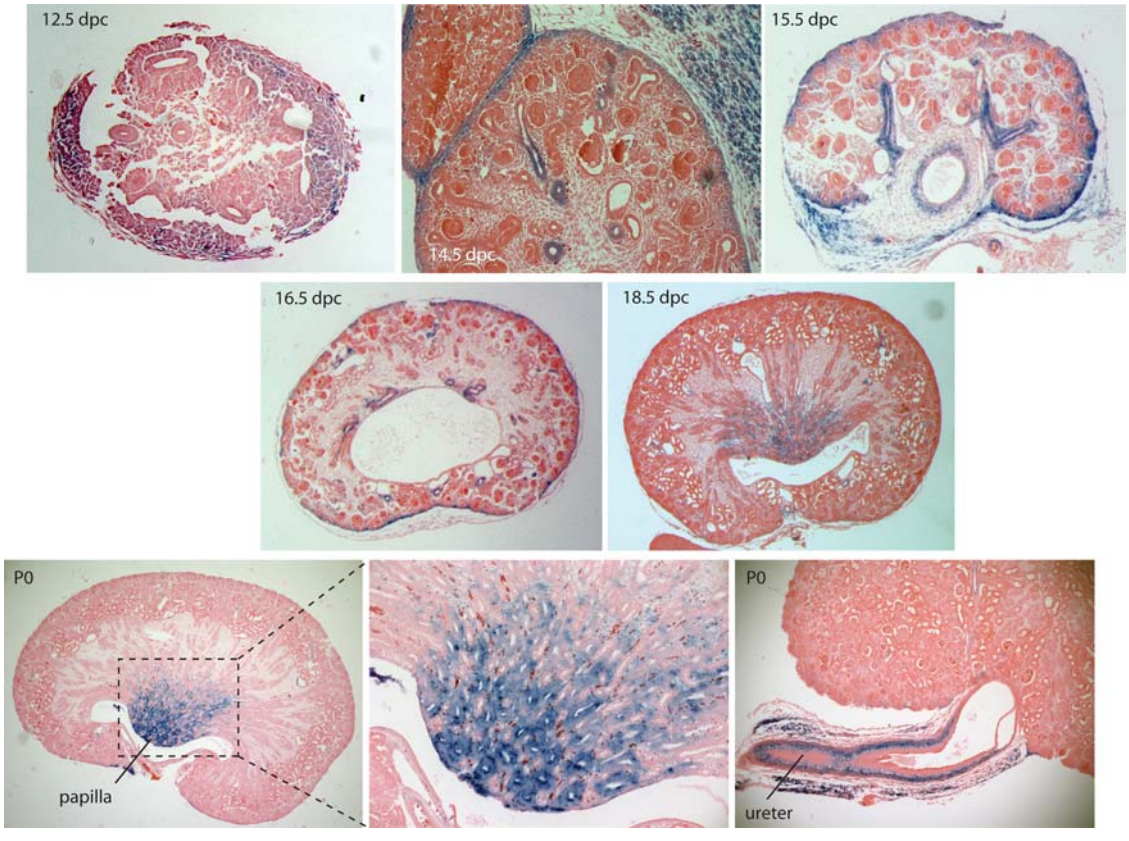

Figure 2. Esrrg immunohistochemistry on sectioned embryonic mouse kidney. Photomicrographs of kidney sections counterstained with eosin (pink) and Esrrg is detected with NBT/BCIP (blue). 12.5 dpc staining in early-stage kidneys can only be seen in the peripheral uncondensed metanephric mesenchyme or stroma. 14.5, 15.5, 16.5 dpc: each kidney shows regionally restricted signal in specific ductal epithelia and in the peripheral mesenchyme. 18.5 dpc and P0 (first postnatal day): signal becomes restricted to the renal papilla and the developing ureter.

sinus and the duodenum with faint expression detectable in the ducts within the liver.

Expression of Esrrg during *in vivo* and *in vitro* kidney development

In dissected wild-type embryonic kidneys, expression is observed in the peripheral metanephric mesenchyme towards the outer edge of the developing kidney at 12.5 dpc. In later stages, expression is seen in the capsule, the adrenal gland and a subset of the ductal tissue within the kidney parenchyma, which forms by branching of the ureteric bud. By 15.5 dpc, the ductal staining appears to be localized to the developing collecting ducts (Fig. 2). By 18.5 dpc, the expression is localized to the collecting ducts in the developing renal papilla and this persists in the neonate kidney. From 14.5 dpc, the nephrons are negative for Esrrg staining. There is a clear staining of Esrrg in the ureteric smooth muscle at P0 (Fig. 2). No expression could be seen in the adult mouse kidney sections examined (data not shown).

In vitro culture of wild-type embryonic kidneys was used for more detailed analysis of the expression pattern of Esrrg in the ureteric bud. In this system, Esrrg staining was found to be entirely ductal (Fig. 3A–F). The strongest Esrrg staining partially overlapped with Pax8 in the peripheral ductal tissue (Fig. 3A and C). In most cells, expression of Esrrg and Wt1, a marker for condensing mesenchyme and developing glomeruli, appears to be non-overlapping (Fig. 3B and D). A suggestion of a site-specific change in subcellular distribution of Esrrg was observed; in the proximal ducts, there was apparent staining in the cytoplasmic/sub-membranous compartment of cells (Fig. 3F); however, in the developing nephron, the staining was nuclear (Fig. 3E).

Effect of siRNA knock-down of Ush2a and Esrrg in cultured embryonic kidneys

Pools of siRNAs targeted against either *Esrrg* or *Ush2a* were transfected into explanted mouse embryonic kidneys. *Ush2a* was chosen as a comparator because this is the closest neighbouring gene to *Esrrg*, and *USH2A* is directly disrupted by the 1q41 translocation breakpoint associated with bilateral renal agenesis (6). However, *USH2A* is not a good candidate for this phenotype as homozygous loss-of-function mutations in humans and mice result in hearing loss and retinal degeneration with no renal phenotype (7). Culture of the explants following siRNA transfection revealed a striking growth arrest in the *Esrrg* targeted kidneys that were not seen in *Ush2a* or the mock transfections (Fig. 4A). A statistically significant reduction in the number of nephrons and the number of bud tips was observed in the Esrrg targeted tissues (Fig. 4B).

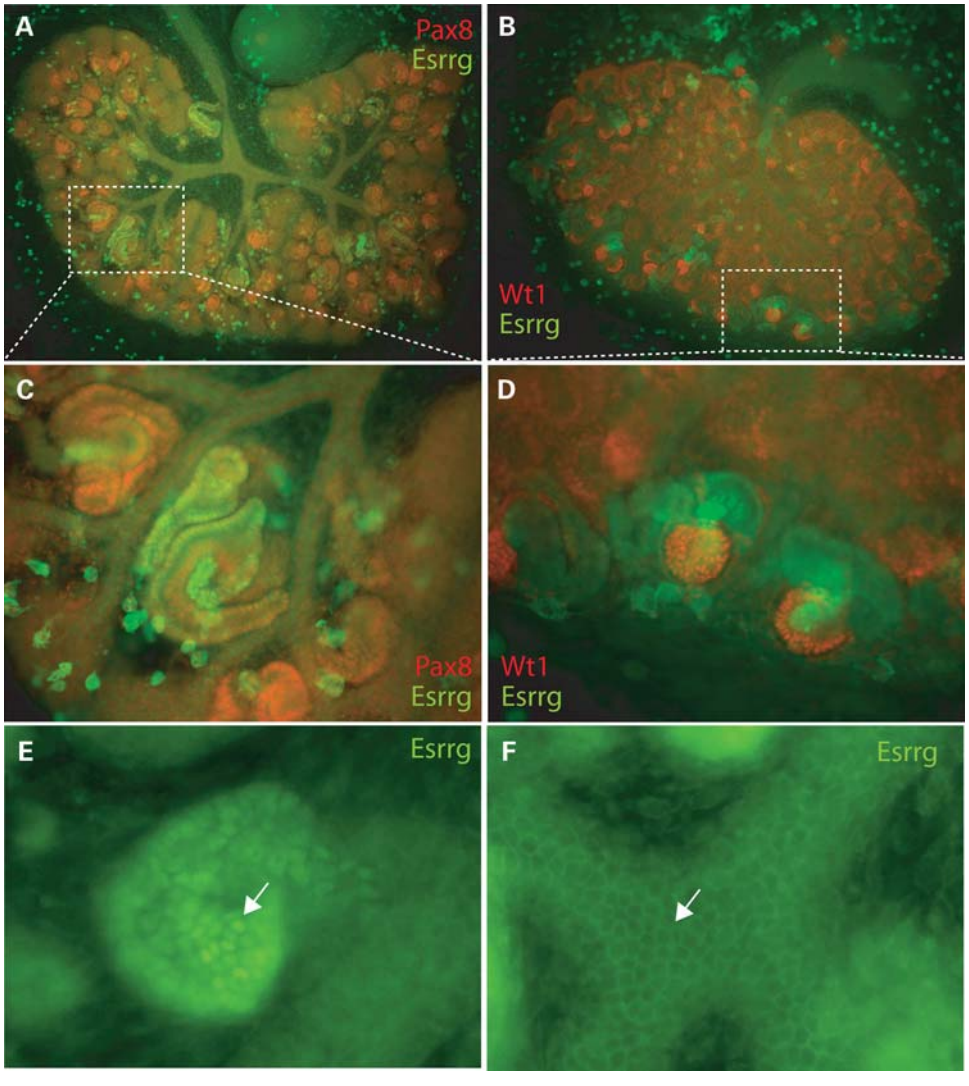

Figure 3. Immunohistochemistry of cultured embryonic mouse kidney. Photomicrographs of embryonic mouse kidneys collected at 11.5 dpc and cultured for 3 days. (**A** and **B**) Representative cultured wild-type kidney stained by co-immunofluorescence with antibodies for Esrrg (green, A and B), Pax8 (red, A) and Wt1 (red, B). Esrrg staining is ductal with stronger staining apparent at the periphery. Esrrg partially overlaps with Pax8 in the peripheral ductal tissue (**C**), but was generally distinct from that of Wt1, which marks the developing glomeruli (**D**). A possible site-specific phenomenon was observed in the subcellular distribution of Esrrg; in the central ducts, the staining was diffuse suggesting cytoplasmic or sub-membranous distribution (**E**), but the staining was clearly nuclear (**F**) in the developing nephron.

Effect of a specific Esrrg agonist on cultured embryonic kidneys

Specific agonists for Esrrg have been developed (13). We used one of these, GSK4716, to examine the effect of constitutional activation of Esrrg in cultured embryonic kidneys. Compared with unexposed control embryos, there was a dose-dependent developmental anomaly evident from 2 μM concentration GSK4716. At 10 μM concentration, all the exposed kidneys showed a severe developmental anomaly characterized by reduced size and abnormality in ductal morphogenesis (Fig. 5).

Kidney development in Esrrg-deficient animals

We first examined 17 dpc embryonic kidneys dissected from wild-type, and *Esrrg*$^{+/-}$ and *Esrrg*$^{-/-}$ littermates were imaged by optical projection tomography (OPT). Digital reconstructions of each kidney were visualized in 3D and midline digital sections chosen for each kidney. This showed a clear morpholgical difference between the *Esrrg*$^{-/-}$ kidneys and those from heterozygous or wild-type embryos (Fig. 6). The most striking difference was the flattening of the region of the papilla leading to an increase in luminal volume in 6/6 the mutant kidneys. A similar change was seen in only 1/8 of the wild-type embryos and 1/6 of the heterozygous embryos. Quantitation of the luminal volume of whole kidneys and the ratio of lumen to renal parenchyma showed the knock-out (KO) embryos to be clearly different from their heterozygous and wild-type littermates.

Histopathological examination using sections from the same Esrrg$^{-/-}$ embryonic kidneys, as shown in Figure 6, showed marked distortion of normal medullary architecture (Fig. 7D

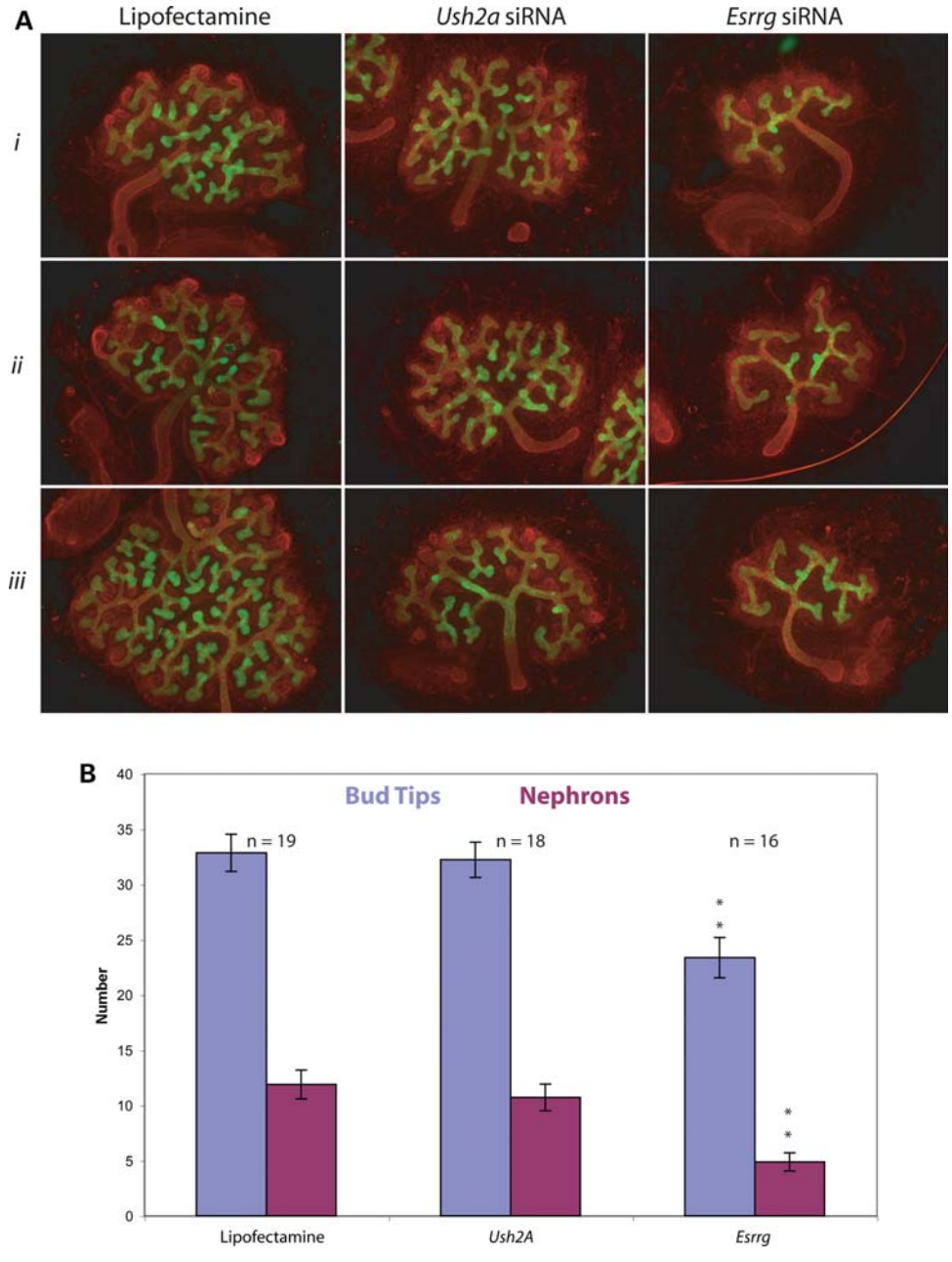

Figure 4. siRNA knock-down in cultured embryonic mouse kidney. siRNA experiments. (**A**) Photomicrographs showing three representative cultured kidneys stained with laminin (red) and calbindin (green) following either mock transfection (lipofectamine) or transfections with pools of siRNA molecules targeted to *Ush2a* or *Esrrg*. No difference is apparent between lipofectamine- and Ush2a-treated kidneys, but kidneys exposed to Esrrg siRNA are smaller and have fewer ductal branch points. (**B**) Graph showing the quantitative differences in numbers of bud tips (blue) and nephrons (purple). The error bars indicate the 95% confidence intervals and the numbers of kidneys used to generate the data are given above the relevant graph bars.

and F) compared with the wild-type (Fig. 7A–C) in the presence of nearly normal cortical architecture and nephrogenesis (Fig. 7E). The medulla, instead of forming a normal blunt cone projecting into the pelvis, forms a concave disc beneath the cortex over a widely dilated pelvis. There was no indication of hydronephrosis, as the ureter is not dilated (Fig. 7D). However, the *Esrrg*$^{-/-}$ cortex shows the same maturational gradient as the wild-type from condensation through tubular maturation (Fig. 7E). Glomerular maturation appeared slightly retarded. The medulla, although architecturally abnormal, contains radiating collecting ducts, primitive loops of Henle and palisades of interstitial cells (Fig. 7F). Both the quantitative and histological analyses are consistent with a diagnosis of specific papillary agenesis.

In order to assess the genesis of these morphological anomalies, kidneys were examined at an earlier developmental stage (14.5 dpc). No difference could be detected between any of the three genotypes on histological examination or using immunohistochemical assays to assess proliferation or apoptosis (Fig. 8).

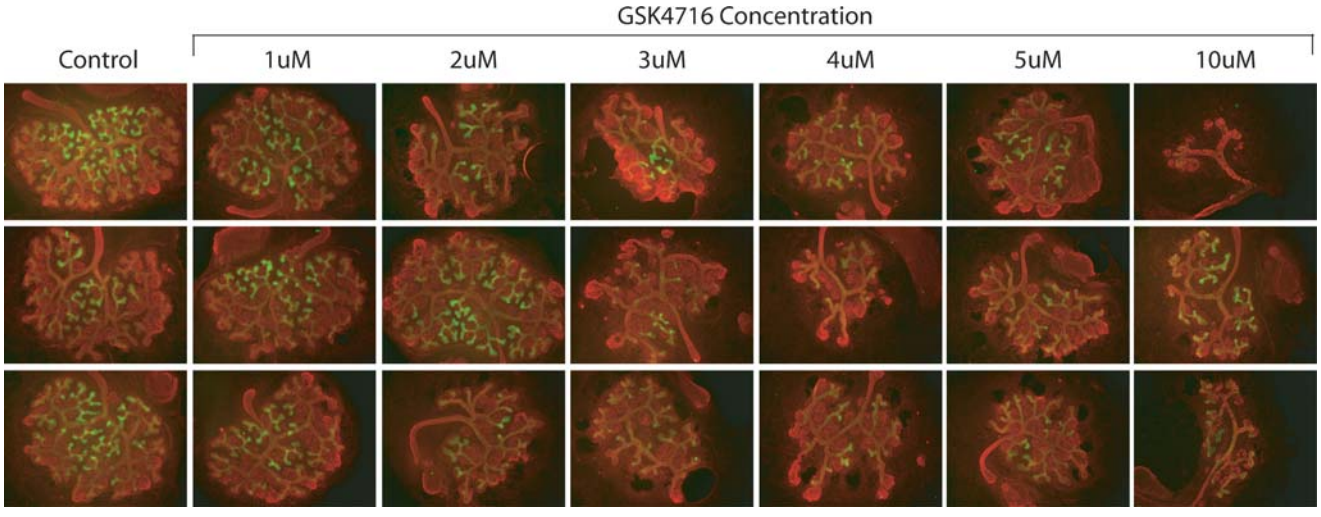

Figure 5. The effect of the Esrrg agonist GSK4716 on cultured embryonic mouse kidney. Effect of exposure to GSK4716. Photomicrographs showing three representative cultured kidneys stained with laminin (red) and calbindin (green) exposed to either none (control) or increasing concentrations (1–10 μM) of the Esrrg agonist GSK4716. At 10 μM concentration, there is a severe developmental anomaly in the exposed embryos with an apparent dose-dependent effect at lower concentrations.

DISCUSSION

Breakpoint mapping of *de novo*, apparently balanced reciprocal translocation, has proven to be an efficient method of identifying the genetic basis of human malformations (14,15). We have recently mapped the breakpoints of a t(1;2)(q41;p25.3) associated with isolated bilateral renal agenesis. This analysis suggested that misregulation of the *ESRRG* gene that mapped close to the chromosome 1q41 breakpoint was a plausible candidate developmental genetic mechanism for the kidney malformation in this case on the basis of striking site-specific expression in the 14.5 dpc embryonic mouse kidney.

Here we have sought to clarify the non-redundant role of ESRRG in kidney development. Immunohistochemical analysis shows that Esrrg is widely expressed in a site-specific manner during mouse embryogenesis. The earliest expression is seen in the developing heart from 9.5 dpc. Expression is also seen in a sub-population of head mesenchyme. From 11.5 dpc, it is striking that several tubular/ductal structures strongly express Esrrg; the Wolfian duct and urogenital sinus, the lung bud and the duodenum. Weaker expression is seen in hepatic ducts. During the development of the metanephic kidney, expression is first seen in the peripheral stroma surrounding the invading ureteric bud. The subsequent expression is ductal and is strikingly regionally restricted. It is intriguing that the subcellular distribution of Esrrg is clearly nuclear in the developing nephrons of the cultured embryonic kidney explants with a suggestion that there is lower level expression in the proximal ductal tissue that is cytoplasmic or submembranous. It will be interesting to identify the molecular basis of this nuclear translocation and any resulting transcriptional response. However, on the basis of the phenotype in *Esrrg*$^{-/-}$ mice, it is very unlikely that this gene product has a non-redundant role in nephron development.

We also provide *in vitro* and *in vivo* evidence for a non-redundant role for Esrrg in kidney development. The siRNA transfections of explant mouse embryo kidney cultures yielded a severe phenotype consistent with an interruption of ductal branching. This phenotype has been confirmed as specific by using a second, independent pool of three siRNA targeting different regions of Esrrg (data not shown). No effect is seen on kidney development using siRNA targeted against the neighbouring gene in both the mouse and human genome, *Ush2a/USH2A*. We show a remarkably similar, dose-dependent phenotype associated with pharmacological activation of ESRRG using a specific agonist, GSK4716. It is, however, important to acknowledge that the specificity of small molecule agonists may be tissue and/or species specific, and these results must be interpreted with some caution.

More convincing evidence for a non-redundant role during kidney development comes from the targeted KO of *Esrrg* in the mouse (16). The targeted mutation removes most of the DNA binding domain of Esrrg coded for in exon 2 and replaces this with an in-frame, promotorless beta-galactosidase cassette. *Esrrg*$^{-/-}$ mice die perinatally and have hyperlactataemia, a cardiomyopathy and a cardiac conduction defect. Transcriptome analysis of the cardiac tissue from affected homozygotes revealed abnormalities in key mitochondrial genes. There was no suspicion of a renal phenotype in these mice. In view of the results obtained from the siRNA experiments, we decided to investigate the kidneys of the *Esrrg*$^{-/-}$ by detailed histology and morphometry. This showed a very site-specific developmental anomaly of the renal papilla in the KO mice compared with heterozygous and wild-type littermates. At the level of OPT analysis, the kidney phenotype was suggestive of fetal hydronephrosis. Recent animal model work has highlighted abnormalities in ureteric peristalsis as an important cause of fetal hydronephrosis (17,18), and Esrrg staining is evident in the musculature of the ureter (Fig. 2). However, on histological analysis, there was no evidence of increased pressure—in particular, there was no evidence of dilation of the collecting duct. We thus consider it likely that the *Esrrg* KO mice have agenesis of the papilla as a primary malformation rather than a dysplastic effect secondary to increased hydrostatic pressure within the ductal system.

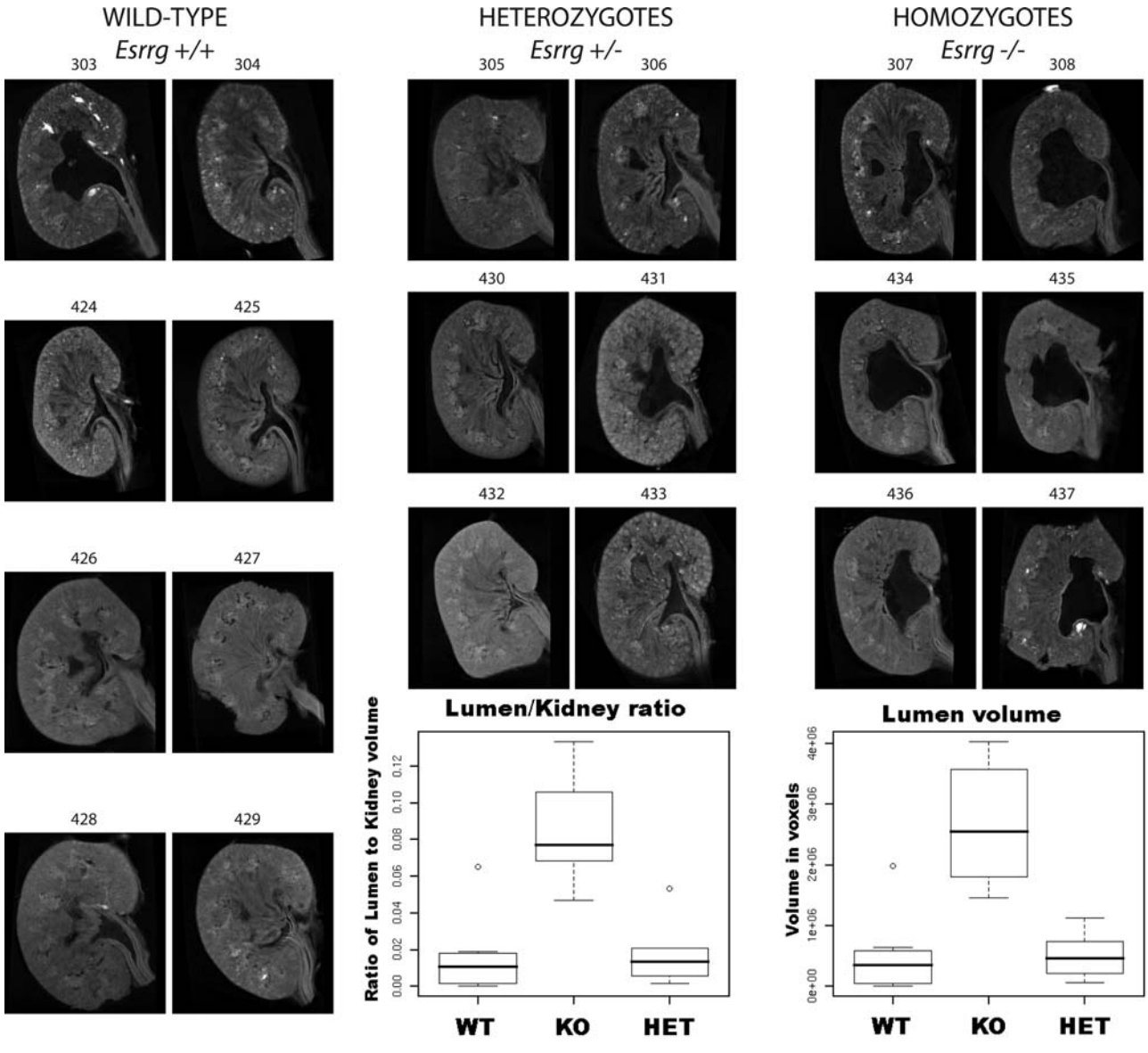

Figure 6. Quantitative analysis of Esrrg$^{-/-}$ mouse embryonic kidneys using OPT imaging. Digital sections from OPT scans of paired 17 dpc embryonic kidneys dissected from littermates of Esrrg$^{+/-}$/Esrrg$^{+/-}$ matings. Eight kidneys from four wild-type embryos (WT), six kidneys from three Esrrg$^{+/-}$ embryos (HET) and six kidneys from three Esrrg$^{-/-}$ embryos (KO) are shown in midline saggital plane defined by analysis of the 3D digital image. The graph shows the range (box), mean (solid line) and error bars (dotted lined) for each genotype group of the luminal volume (right-hand graph) and ratio of lumen to kidney parenchyma for whole kidneys.

The primary function of the renal papilla is thought to be in final maximal concentration of urine (19,20). Currently, it would not be possible to test the *Esrrg*$^{-/-}$ mice for defects in urine concentration in view of the early mortality, but this may be possible in a conditional KO model.

The onset of the morphological change *in vivo* can be timed between 14.5 and 17 dpc. At 14.5 dpc, the KO kidneys are histologically indistinguishable from the wild-type. There was no obvious defect in either proliferation or apoptosis seen in the 14.5 dpc KO kidneys. The renal papilla cannot be visualized at this stage and the 14.5 dpc kidneys are too small for accurate dissection for OPT analysis of the ductal branch patterns. Thus, the developmental basis of the papilla agenesis at 17 dpc is not clear. It is possible that alteration in the number or position of early branch point in the ureteric duct is altered or that cell movement processes such as convergent extension are impaired.

We could not find reports of any equivalent human malformation, although congenital overgrowth of the renal papilla has been rarely reported (21–24). We could find seven mouse mutants with 'abnormal kidney papilla morphology' listed in MGI including inactivation of angiotensin or its receptors (Agt, Agtr1a and Agtr1b), aquaporin (Aqp2), Cdkn1c, Fgf7, Lepr and Adamts1. It will be interesting to determine if any or all of these genes turn out to be transcriptionally controlled by Esrrg. Most of these mutations were associated with more extensive renal and extrarenal problems; however, it is interesting that mutations in AQP2 cause

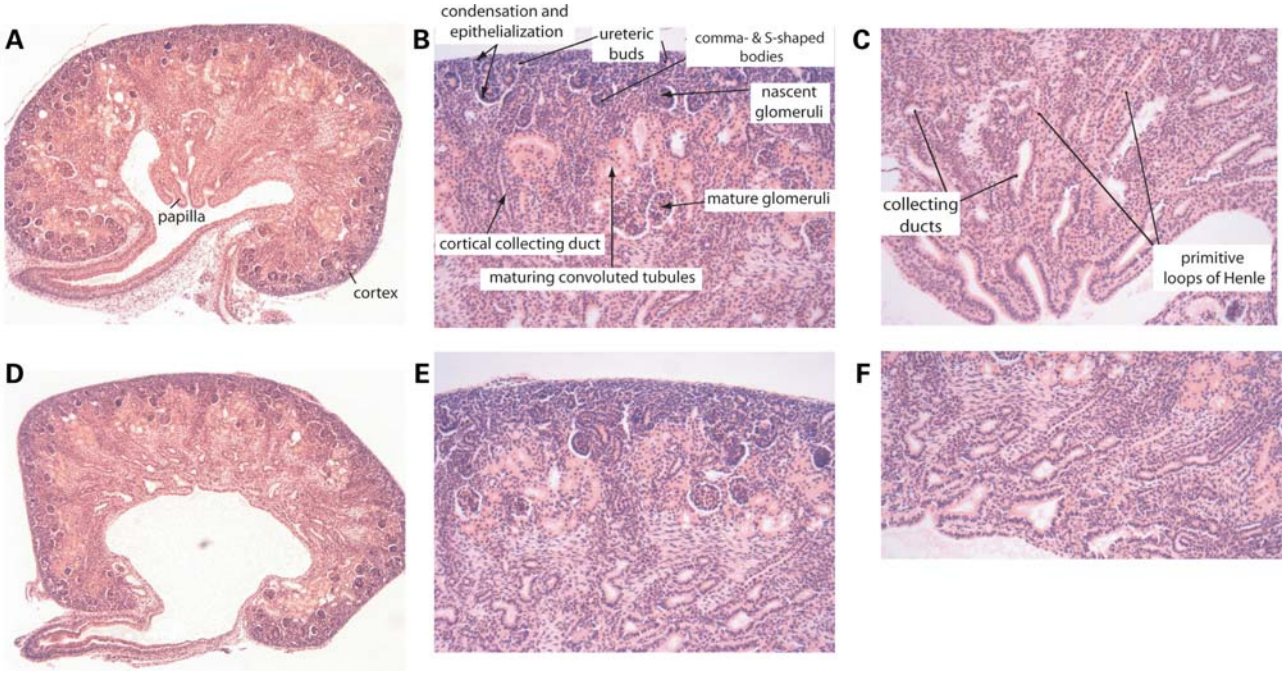

Figure 7. Pathological features of Esrrg$^{-/-}$ mouse embryonic kidneys. Photomicrographs of sections from wild-type (**A**, **B**, **C**) and Esrrg$^{-/-}$ (**D**, **E**, **F**) littermate 17 dpc embryos. (A) The wild-type can be clearly divided into an outer cortex containing the vast majority of developing glomeruli and an inner medullary region in which a blunt papilla is projecting into a mildly dilated pelvis. (B) The wild-type cortex shows a maturational gradient of nephrogenesis from subcapsular condensation of metanephric mesenchyme around ureteric buds, slightly deeper epithelialization, early morphogenesis (comma and s-shaped bodies), nascent glomeruli at the outer third of the cortex and maturing glomeruli and maturation of convoluted tubules in the deeper cortex. (C) The wild-type medulla, in addition to prominent radiating collecting ducts, contains scattered primitive loops of Henle. Interstitial mesenchymal cells are plump fusiform cells beginning to form parallel arrays. (D) The Esrrg$^{-/-}$ kidney has a marked distortion of the medullary architecture with nearly normal cortical architecture and nephrogenesis. The medulla, instead of forming a normal blunt cone projecting into the pelvis, forms a concave disc beneath the cortex over a widely dilated pelvis. The ureter, however, is not dilated. (E) The cortex shows the same maturational gradient as the wild-type from condensation through tubular maturation. Glomerular maturation appears slightly retarded. (F). The medulla contains radiating collecting ducts, primitive loops of Henle and palisades of interstitial cells but lacks a papilla.

nephrogenic diabetes insipidus and mutations in either AGT or AGTR1A cause renal tubular dysgenesis in humans. These phenotypes may provide informative cohorts in which to look for mutations in *ESRRG*.

Finally, to return to our original hypothesis, it seems unlikely, given the mild and apparently asymptomatic phenotype we have observed in the mouse, that inactivating mutations of ESRRG are the sole cause of the bilateral renal agenesis in the t(1;2)(q41;p25.3) case. It may be that mice are simply much more tolerant of Esrrg dosage than humans. However, it is plausible, given the effect of the Esrrg-agonist on the cultured kidney, that aberrant activation of ESRRG occurs via gain of a renal enhancer element or loss of a specific repressor may be a causative *cis*-regulatory mutation in that case. Important future work will include investigating CAKUT cases for copy number variants that may result in duplication of *ESRRG* transcription unit or of enhancers controlling the renal expression of this gene.

MATERIALS AND METHODS

Immunohistochemical analysis

Four to 6 μm sections from paraformaldehyde-fixed, paraffin-embedded wild-type CD1 mouse embryos were used for immunohistochemical localization of Esrrg with a rabbit polyclonal antiserum (AbCam, cat ab12988) at a dilution of 1 in 500. De-waxed sections were boiled in 10 mM citrate buffer twice for 30 s and left to cool in the buffer for 20 min. Ten percent heat-inactivated sheep serum in PBS was applied to reduce non-specific binding. The slides were incubated in the primary antibody at 4°C overnight in a humidified chamber, washed and the secondary antibody (biotinylated anti-rabbit IgG, 1 in 1000) applied for 1 h at room temperature. Detection was performed using the Vector Lab ABC kit and NBT/BCIP and sections were counterstained with eosin. The antibody staining protocols used to assess proliferation (1/800 Phospho-Histone H3, Cell Signaling, 9701) and apoptosis (1/200 Cleaved Caspase-3, Cell Signaling, 9661) were performed using a minor modification of a previously reported method (25). The modifications were that sections were microwaved in TEG buffer (1.211 g Tris, 0.190 g EGTA in distilled water to 1000 ml, pH 9.0) using a pressure cooker for 4 min and detected using diaminobenzidine (Kem-En-Tec Diagnostics A/S, Denmark) and the sections were counter stained with Mayer's haemalum (Fisher Scientific).

On cultured embryonic kidneys, the following primary antibodies and dilutions were used: Laminin 1/200 (Sigma, L9393), Calbindin 1/200 (Abcam, ab9481), Esrrg 1/200 (R&D Systems, PP-H6812-00), WT1-F6 1/100 (Santa Cruz, sc7385) and Pax8 1/200 (ProteinTech, 10336-1-AP). Cultured kidneys were incubated in primary antibody overnight at 4°C. The

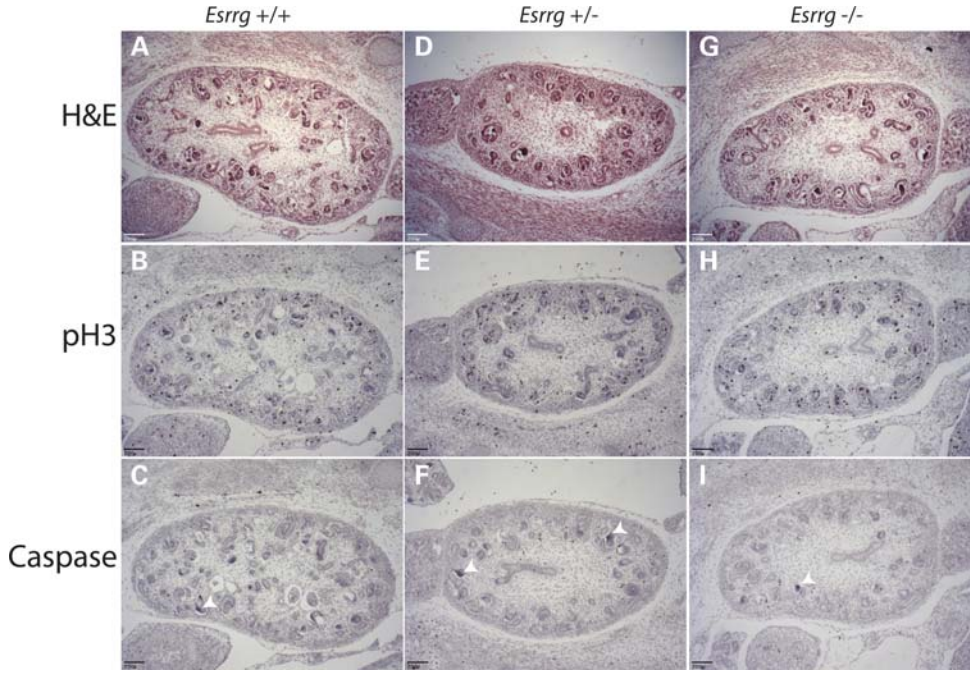

Figure 8. Esrrg$^{-/-}$ mouse embryonic kidneys appear normal at 14.5 dpc. Photomicrographs of sections from wild-type (**A**, **B**, **C**), heterozygous (**D**, **E**, **F**) and Esrrg$^{-/-}$ (**G**, **H**, **I**) littermate 14.5 dpc embryos. These sections have been stained with H&E (A, D, G), an antibody that detects phosphorylated histone H3 as a marker of cells undergoing mitosis (pH 3; B, E, H) and an antibody that detects activated caspase 3 as a marker for apoptosis (Caspase; C, F, I). No obvious differences could be detected between the genotypes in any of the staining groups. There were relatively few apoptotic cells in the kidney at this stage and those that were present localized to the ducts (white arrowheads).

following day, six 1 h washes in PBST (PBS with 1% Triton X-100) were carried out at room temperature. Secondary antibodies: Alexa 594 donkey anti-rabbit IgG 1/400 (Invitrogen, A21207) and Alexa 488 donkey anti-mouse 1/400 (Invitrogen, A21202) were incubated overnight at 4°C, followed by six 1 h washes in PBST as above. The kidneys were mounted in Vectashield mounting medium for fluorescence (Vector Labs, H-100). Immunofluorescence was observed and recorded on an imaging system comprising a Coolsnap HG CCD camera (Photometrics Ltd, Tucson, AZ, USA) and Zeiss Axioplan II fluorescence microscope with Plan-neofluar objectives. Image capture and analysis were performed using in-house scripts written for IPLab Spectrum (Scanalytics Corp., Fairfax, VA, USA).

In vitro mouse embryonic kidney culture

Kidneys at the T-bud stage of development were isolated from 11.5 dpc wild-type embryos (cd1 × cd1). These were cultured on 0.4 μm pore size Transwell filters (Costar, 3450). The kidneys were cultured at 37°C with 5% CO_2 in Minimum Essential Medium Eagle medium (Sigma M5650) supplemented with 10% newborn calf serum and 1% penicillin and streptomycin. Kidneys were fixed in ice-cold methanol for 10 min, washed briefly in PBS and blocked in PBS, BSA and sodium azide overnight at 4°C.

siRNA knock-down in cultured mouse embryonic kidneys

RNAi in kidney organ cultures were performed as previously reported (26) with some modifications. Kidneys at the T-bud stage of development were isolated from 11.5 dpc wild-type embryos (cd1 × cd1) and cultured on 0.4 μm pore size Transwell filters (Costar, 3450). Two separate mixes were prepared, the first one consisting of 30 μl of total siRNA (20 μM stock) and 1150 μl of Improved MEM, Zinc Option (Gibco 10373) supplemented with 10 μg/ml iron-loaded human transferrin (Sigma) medium. siRNAs were available commercially from Invitrogen (Esrrg siRNA, 10620312) and Ambion (Ush2a control siRNA, AM16704). The second mix consisted of 69 μl of Lipofectamine-2000 (Invitrogen) in 350 μl of Improved MEM, Zinc Option medium (Gibco 10373) supplemented with 10 μg/ml of iron-loaded human transferrin. These mixes were incubated for 10 min at room temperature and subsequently the lipofectamine mix was added dropwise to the siRNA mix. After a further 20 min incubation at room temperature, 1.5 ml was placed in the bottom of the transwell, and a 100 μl was pipetted gently on top of the kidneys. Following 24 h incubation, the medium was changed to Minimum Essential Medium Eagle (Sigma M5650) with 10% newborn calf serum, and 1% penicillin and streptomycin, and the kidneys cultured for a further 2 days. The kidneys were cultured at 37°C with 5% CO_2.

Esrrg agonist application to cultured mouse embryonic kidneys

Kidneys at the T-bud stage of development were isolated from 11.5 dpc wild-type embryos (CD1 × CD1), and cultured as described above. Esrrg agonist, GW4716 (Sigma), was dissolved in ethanol and added to Minimum Essential Medium

Eagle medium (Sigma M5650) supplemented with 10% newborn calf serum and 1% penicillin and streptomycin at concentrations of 0–5 and 10 μM. The same total volume of ethanol was used in each condition. Kidneys were cultured at 37°C with 5% CO_2 for 3 days. The kidneys were then fixed in ice-cold methanol for 10 min, washed briefly in PBS and blocked in PBS, BSA-Azide overnight at 4°C, before staining with laminin and calbindin.

OPT and quantitative analysis

Mouse embryonic kidneys were fixed in 4% paraformaldehyde overnight, mounted in 1% agarose, dehydrated in methanol and then cleared overnight in BABB (1 part Benzyl Alcohol: 2 parts Benzyl Benzoate) (27). Each kidney was separately imaged using a Bioptonics OPT Scanner 3001 (Bioptonics, UK) with tissue autofluorescence (excitation 425 nm/emission 475 nm) used to capture the anatomy. The resulting images were reconstructed using Bioptonics proprietary software. The resulting 3D digital representations were imported into Amira for digital sectioning and quantitative assessments.

ACKNOWLEDGEMENTS

We would like to thank Professor Veronica van Heyningen for her helpful advice and support of this project and Dr Shrobona Bhattacharya for help with scanning and staining the mouse embryos.

Conflict of Interest statement. None declared.

FUNDING

This work was supported by the Medical Research Council Human Genetics Unit. Funding to pay the Open Access publication charges for this article was provided by MRC Human Genetics Unit.

REFERENCES

1. Hiruma, T. and Nakamura, H. (2003) Origin and development of the pronephros in the chick embryo. *J. Anat.*, **203**, 539–552.
2. O'Rahilly, R. and Müller, F. 1987. *Developmental Stages in Human Embryos*. Carnegie Institution of Washington.
3. Costantini, F. (2006) Renal branching morphogenesis: concepts, questions, and recent advances. *Differentiation*, **74**, 402–421.
4. Dressler, G.R. (2006) The cellular basis of kidney development. *Annu. Rev. Cell Dev. Biol.*, **22**, 509–529.
5. Woolf, A.S., Price, K.L., Scambler, P.J. and Winyard, P.J. (2004) Evolving concepts in human renal dysplasia. *J. Am. Soc. Nephrol.*, **15**, 998–1007.
6. Joss, S., Howatson, A., Trainer, A., Whiteford, M. and FitzPatrick, D.R. (2003) De novo translocation (1; 2)(q32; p25) associated with bilateral renal dysplasia. *Clin. Genet.*, **63**, 239–240.
7. Harewood, L., Liu, M., Keeling, J., Howatson, A., Whiteford, M., Branney, P., Evans, M., Fantes, J. and Fitzpatrick, D.R. (2010) Bilateral renal agenesis/hypoplasia/dysplasia (BRAHD): postmortem analysis of 45 cases with breakpoint mapping of two de novo translocations. *PLoS ONE*, **5**, e12375.
8. Huppunen, J., Wohlfahrt, G. and Aarnisalo, P. (2004) Requirements for transcriptional regulation by the orphan nuclear receptor ERRgamma. *Mol. Cell Endocrinol.*, **219**, 151–160.
9. Yu, D.D. and Forman, B.M. (2005) Identification of an agonist ligand for estrogen-related receptors ERRbeta/gamma. *Bioorg. Med. Chem. Lett.*, **15**, 1311–1313.
10. Wang, L., Zuercher, W.J., Consler, T.G., Lambert, M.H., Miller, A.B., Orband-Miller, L.A., McKee, D.D., Willson, T.M. and Nolte, R.T. (2006) X-ray crystal structures of the estrogen-related receptor-gamma ligand binding domain in three functional states reveal the molecular basis of small molecule regulation. *J. Biol. Chem.*, **281**, 37773–37781.
11. Kim, Y., Koh, M., Kim, D.K., Choi, H.S. and Park, S.B. (2009) Efficient discovery of selective small molecule agonists of estrogen-related receptor gamma using combinatorial approach. *J. Comb. Chem.*, **11**, 928–937.
12. Huang, Z., Fang, F., Wang, J. and Wong, C.W. (2010) Structural activity relationship of flavonoids with estrogen-related receptor gamma. *FEBS Lett.*, **584**, 22–26.
13. Zuercher, W.J., Gaillard, S., Orband-Miller, L.A., Chao, E.Y., Shearer, B.G., Jones, D.G., Miller, A.B., Collins, J.L., McDonnell, D.P. and Willson, T.M. (2005) Identification and structure-activity relationship of phenolic acyl hydrazones as selective agonists for the estrogen-related orphan nuclear receptors ERRbeta and ERRgamma. *J. Med. Chem.*, **48**, 3107–3109.
14. Fantes, J., Ragge, N.K., Lynch, S.A., McGill, N.I., Collin, J.R., Howard-Peebles, P.N., Hayward, C., Vivian, A.J., Williamson, K., van Heyningen, V. and FitzPatrick, D.R. (2003) Mutations in SOX2 cause anophthalmia. *Nat. Genet.*, **33**, 461–463.
15. FitzPatrick, D.R., Carr, I.M., McLaren, L., Leek, J.P., Wightman, P., Williamson, K., Gautier, P., McGill, N., Hayward, C., Firth, H. *et al.* (2003) Identification of SATB2 as the cleft palate gene on 2q32-q33. *Hum. Mol. Genet.*, **12**, 2491–2501.
16. Alaynick, W.A., Kondo, R.P., Xie, W., He, W., Dufour, C.R., Downes, M., Jonker, J.W., Giles, W., Naviaux, R.K., Giguere, V. and Evans, R.M. (2007) ERRgamma directs and maintains the transition to oxidative metabolism in the postnatal heart. *Cell Metab.*, **6**, 13–24.
17. Caubit, X., Lye, C.M., Martin, E., Core, N., Long, D.A., Vola, C., Jenkins, D., Garratt, A.N., Skaer, H., Woolf, A.S. and Fasano, L. (2008) Teashirt 3 is necessary for ureteral smooth muscle differentiation downstream of SHH and BMP4. *Development*, **135**, 3301–3310.
18. Chang, C.P., McDill, B.W., Neilson, J.R., Joist, H.E., Epstein, J.A., Crabtree, G.R. and Chen, F. (2004) Calcineurin is required in urinary tract mesenchyme for the development of the pyeloureteral peristaltic machinery. *J. Clin. Invest.*, **113**, 1051–1058.
19. Gobe, G.C. and Axelsen, R.A. (1984) Impaired renal concentrating capacity in the rat after surgical resection of the papilla. *Aust. J. Exp. Biol. Med. Sci.*, **62**, 373–379.
20. Ma, Y.H. and Dunham, E.W. (1991) Rat renal papillary release of hypotensive substances *in vitro*. *J. Hypertens.*, **9**, 761–770.
21. Whitaker, R.H. and Edwards, D. (1969) Congenital hypertrophy of a renal papilla. *Br. J. Urol.*, **41**, 287–289.
22. Wolfson, J.J. and Stowell, D.W. (1969) Aberrant renal papilla simulating an intrarenal mass. Report of two cases. *Radiology*, **93**, 812–814.
23. Anagnostopoulos, C., Galiez, B., Katz, M. and Blery, M. (1985) Aberrant renal papilla. Apropos of a case. *J. Radiol.*, **66**, 393–395.
24. Sala Barange, X., Mandana, A. and Bonet, I. (1987) Aberrant renal papilla. Description of a new sign and review of the literature. *J. Urol. (Paris)*, **93**, 369–371.
25. Tauris, J., Christensen, E.I., Nykjaer, A., Jacobsen, C., Petersen, C.M. and Ovesen, T. (2009) Cubilin and megalin co-localize in the neonatal inner ear. *Audiol. Neurootol.*, **14**, 267–278.
26. Davies, J.A., Ladomery, M., Hohenstein, P., Michael, L., Shafe, A., Spraggon, L. and Hastie, N. (2004) Development of an siRNA-based method for repressing specific genes in renal organ culture and its use to show that the Wt1 tumour suppressor is required for nephron differentiation. *Hum. Mol. Genet.*, **13**, 235–246.
27. Sharpe, J., Ahlgren, U., Perry, P., Hill, B., Ross, A., Hecksher-Sorensen, J., Baldock, R. and Davidson, D. (2002) Optical projection tomography as a tool for 3D microscopy and gene expression studies. *Science*, **296**, 541–545.